Journal of Physical and Theoretical Chemistry
of Islamic Azad University of Iran, 12 (2) 87-95: Summer 2015
(J. Phys. Theor. Chem. IAU Iran)
ISSN 1735-2126

Effect of the hydrothermal treatment, HCl purification and annealing temperature on the structure and the morphology of TiO_2 nanotubes

Samuel Alejandro Lozano Morales*, Héctor Romero Santana and Miguel Ángel López Zavala

Water Center for Latin America and the Caribbean, ITESM

Received February 2015; Accepted March 2015

ABSTRACT

Recently titanium oxide nanotubes (TiO_2) are obtained by hydrothermal alkaline synthesis; where synthesis temperature and pressure, concentrations of NaOH and HCl, and annealing temperature are important parameters in the formation, purification and stability of the nanotubes structure. In this work, the effect of the hydrothermal treatment, the purification and the annealing temperature on the formation process, structure and morphology of TiO_2 nanotubes was investigated. X-Ray diffraction (XRD), transmission electron microscopy (TEM), and EDS (energy dispersive X-ray spectroscopy) analysis were conducted to describe the formation and characterization of the structure and morphology of the nanotubes. From the analysis of results it was found that the hydrothermal treatment of the precursor nanoparticles of TiO_2 and the purification with a HCl solution are essential to form and define the structure of the nanotubes. The hydrothermal treatment induces a change in the crystalline structure of the precursor nanoparticles from anatase phase to an orthorhombic phase which characterizes the titanate structure. The purification contributes to the formation of high purity nanotubes due to a Na exchange from the titanate structure to the HCl solution. The annealing temperature affects the morphology and the dimensions of the nanotubes structure. Annealing temperatures in the range of 400^{o}C and 600^{o}C are optimum to maintain a very stable tubular morphology of nanotubes. Temperatures greater than 600^{o}C change the morphology of nanotubes from tubular to an irregular structure of nanoparticles with a size bigger than that of the precursor material, i.e., the crystalline structure changes from anatase phase to rutile phase causing the destruction of the nanotubes.

Keywords: Nanostructures; Oxides; Chemical synthesis; X-ray diffraction; Thermal expansion.

INTRODUCTION

The1D nanostructures of TiO_2 such as nanotubes, nanocables, and nanobelts, have attracted the attention of researchers because their high potential as catalyst on the fields of electronics, optics, sensing and energy conversion [1,2]. Due to their high surface area compared to bulk material, the nanostructures improve the electron transfer and consequently their efficiency on different applications. These applications require reliable materials with well controlled characteristics such as high

*Corresponding author: alejandrolozanom@itesm.mx

purity, crystallinity, and stability at high temperatures [3]. Currently, the TiO2 nanotubes have been synthesized by sol-gel [4], anodization [5], and molecular assembly [6]. But, using these techniques, low dimensional TiO_2 nanotubes with high crystallinity cannot be produced. Kasuga et al [7] proposed a cheap and safety alkaline hydrothermal method to synthesize nanotubes with high purity [8,9]. They established that the formation of nanotubes of TiO_2 depends on the hydrothermal treatment and the purification process; but, they did not discussed the effect of annealing temperature on the thermal stability, morphology and crystalline structure of nanotubes.

Wang et al. [10], *Kiatkittipong et al.* [11] and *B. Vijayan et al.* [12] found that the annealing temperature is the main parameter which affects the formation of TiO_2nanotubes, but they did not discuss about the morphology and crystallinity. Thus, this work describes the synthesis of TiO_2 nanotubes by hydrothermal process and also evaluates the effect of the annealing temperature on the morphology and crystallinity of the nanotubes.

MATERIAL AND METHOD

Chemical reagents for the synthesis of TiO_2 nanotubes.

All the chemical reagents were analytical grade (Table 1). For the synthesis of TiO_2 nanotubes, the following reagents were used, Degussa P25 nanoparticles (Sigma-Aldrich) with a mixture of anatase (80%) and rutile (20%) phases; sodium hydroxide and hydrochloric acid (from Baker); (and high purity water from Millipore equipment of 0.0001 g was used for weighing. The temperature was controlled by a thermostatic water bath fluctuating to 0.1C

Synthesis of TiO_2 nanotubes

TiO_2 nanotubes were synthesized using a chemical procedure similar to the one proposed by *Kasuga et al*. [7]. As a precursor for this synthesis, 0.3 g of Degussa P25 TiO_2 nanoparticles were used, these nanoparticles were dispersed in to 30 ml of 10 M sodium hydroxide. The solution was stirred vigorously for 2 hours at 30°C. After this time, the solution was warm up in an autoclave at 110°C for 72 h. The product obtained in this step was redispersed in 200 ml of 0.1 M HCl solution for 3 hours. Then, the solution was centrifuged and the solid sample was washed with distilled water until pH was stabilized at 6.7, similar to distilled water pH value. Finally, the samples were dried in a vacuum oven at 80°C for 24 h. The dried sample was divided into three portions and then annealed at 400^{o}C, 600^{o}C and 800°C for 2 hours, respectively.

Structural characterization of TiO_2 nanotubes.

Structural characterization of nanotubes was performed by XRD. A Bruker AXS-D5000 difractometer was used with a wave length λ = 1.5418 Å (Kα), a diffraction angle (2θ) ranging from 5° to 80°, step of 0.020°, scan speed of 0.6 s/step, and a temperature of 30 °C. Powders from calcined samples were prepared by using an agate mortar and then analyzed. Average size, composition and morphology of nanotubes were determined by TEM (model Jeol JSM-5400 LV). The equipment was operated with a 4 nm resolution, a current of 75 mA, a voltage of 5KeV, a working distance of 10 mm, and a pressure of $1.3x10^{-3}$ Pa. The samples were placed in a sample holder and then, a thin film of gold was deposited on the sample surface by sputtering and analyzed by dispersive energy spectroscopy (EDS) with a JEOL JEM 2100 equipment. The equipment was operated at an accelerating

voltage of15 eV, a current of 75 mA, a pressure of $1.3x10^{-3}$ Pa and a working distance of 25 mm.

RESULTS AND DISCUSSION

Structural characteristics of TiO_2 nanotubes

Figure 1 shows the X-ray diffractogram of nanotubes after different treatments. (a) represents the precursor Degussa P25; (b) nanotubes after a hydrothermal treatment at 110°C; (c) annealed nanotubes after purification with a 0.1 M HCl solution; (d) nanotubes after annealing treatment at 400 °C; (e) nanotubes after annealing treatment at 600°C; (f) nanotubes after annealing treatment at 800°C in air for 2 h. This annealing temperatures were proposed to observe the thermal stability of the nanotubes.

As seen in Figure 1a, diffractions were observed at the followings angles 25.37°, 37.96°, 47.93°, 54.04°, 55.37°, 62.75°, 68.82°, 70.53° and 75.11°, which correspond to the crystalline planes (101), (004), (200), (105), (211), (204), (116), (200) and (215) of the anatase phase identified with *JCPDS21-1272 card* [i]. The average size of the nanoparticles was determined by the *Scherrer* formula (equation 1), resulting in a diameter of 24 nm, which corresponds to the values reported by the manufacturer.

$$\phi = \frac{0.9\lambda}{\Delta(2\theta)\cos\theta} \qquad (1)$$

where, λ: Wavelength of the radiation (λ_{Cu}); θ: angle; Φ: Cristal average size.

As observed in Figure 1b, there are three main diffraction peaks located at the diffraction angles (2θ) 9.7°, 29.4° and 48.5°; which differs from those attributed to the anatase phase. This result may suggest that the anatase structure of the precursor nanoparticles has changed. Indeed, the crystalline structure of the samples looks similar to the orthorhombic structure of the titanate (H2Ti3O7), reported by Q. Chen et al [12] and Vijayan et al [14].

The patterns in the Figures 1b y 1c show the same peaks, except at a diffraction angle of 9.7°, where the peak is absent in Figure 1c. This difference is attributed to the collapse of nanotubes due to the exchange of Na present in the nanotubes structure, as reported by the literature [15].

The pattern shown in Figure 1d reveals that some diffraction peaks increase in intensity and are closer to the diffraction planes (101), (004), (210), (105) and (204), similar to those of the anatase phase of the precursor. These results suggest that nanotubes annealed at 400°C recovers the anatase structure of the precursor nanoparticles.

The Figure 1e presents a pattern of anatase structure similar to that of Figure 1d, i.e. anatase structure of nanotubes was stable within the annealing temperature range of 400°C and 600°C. On the contrary, at 800°C the diffraction peaks differ from those observed in the patterns of Figures 1d and 1e, denoting that anatase structure has changed. Indeed, the crystalline structure observed in Figure 1f corresponds to rutile phase according to *JCPDS 01-086-0148 card* [16]. TEM images revealed that nanotubes are destroyed and converted into non uniform nanoparticles at annealing temperatures greater than 600°C.

Morphology of TiO_2 nanotubes

Figure 2 shows a TEM micrograph of the precursor nanoparticles of TiO_2 (Degussa P25). As seen, nanoparticles are not

uniform. According to the histogram (Figure 3) the average size was 25 nm with a standard deviation of 2.83 nm. This result is similar to that obtained with equation 1.

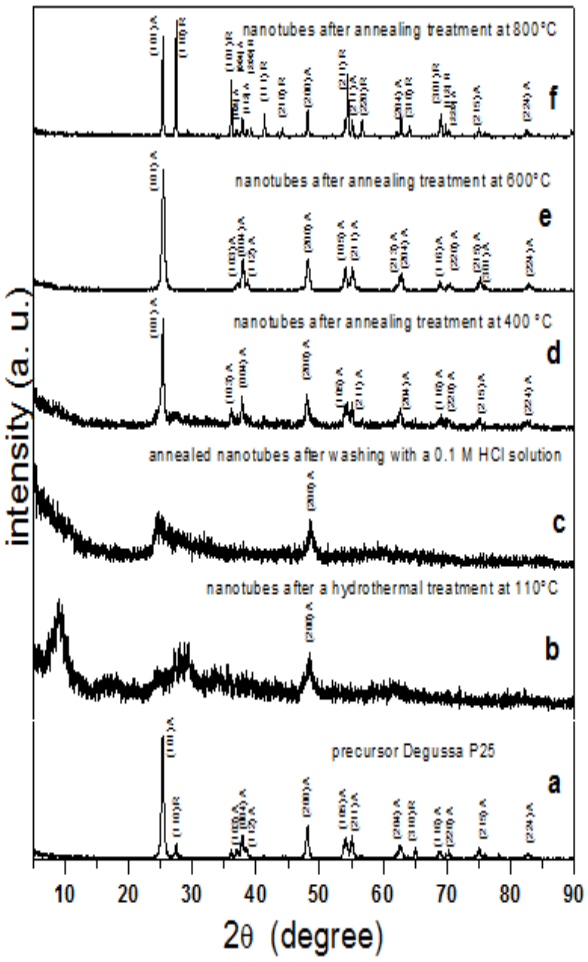

Fig. 1. X-ray diffractogram of nanotubes after different treatments: (a) precursor Degussa P25; (b) nanotubes after a hydrothermal treatment at 110°C; (c) annealed nanotubes after washing with a 0.1 M HCl solution, (d) nanotubes after annealing treatment at 400 °C; (e) nanotubes after annealing treatment at 600°C; (f) nanotubes after annealing treatment at 800°C.

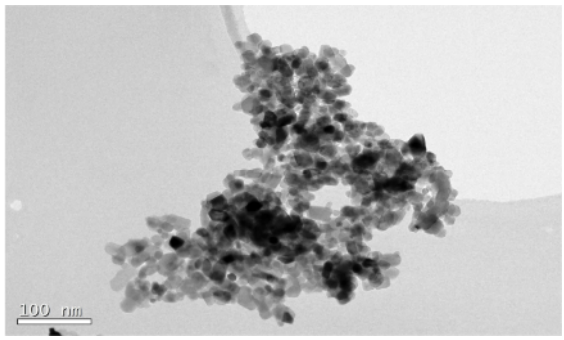

Fig. 2. TEM image of nanoparticles of TiO_2 (Degussa P25).

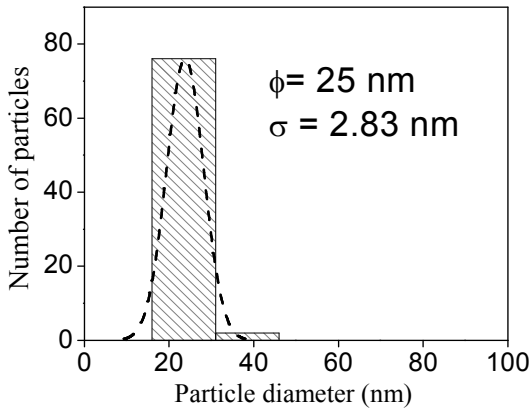

Fig. 3. Average size of TiO2 (Degussa P25) nanoparticles.

Figure 4 shows micrographs of the TEM analysis conducted to precursor nanoparticles after the hydrothermal treatment at 110 °C and 72 hours of reaction time, prior to the purification process. As seen, no tubular structures or particles are observed, but nanosheets structures are clearly seen. According to the formation mechanism [17], if the tubular structure would have been formed, a couple of walls of multiple layers would be observed [18,19]. In Figure 4, the formation of nanosheets (2D) with a random distribution and a nearly curled end was observed. These results differed from those reported in literature that conclude that nanosheets are formed in

reaction times lower than 72 h [20, 21, 22, 23, 24, 25]. According to the formation mechanism of TiO2 nanotubes proposed by Wang et al. [26], 2D nanosheets constitute an intermediate step essential to the formation of nanotubes [27].

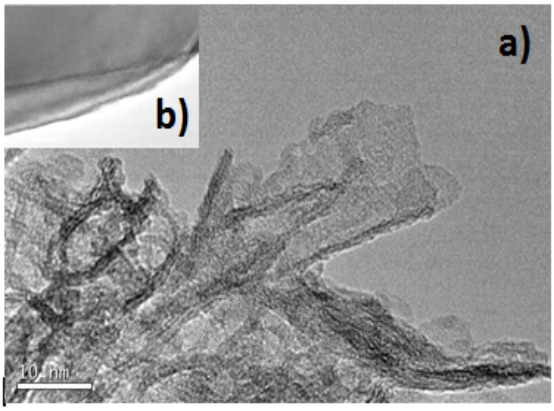

Fig. 4. TEM micrographs of precursor nanoparticles after hydrothermal treatment: (a) nanosheets formation, (b) change of the nanosheets.

Wang et al. [28] found that the purification process and the acidity of the purification solution determine the morphology, length and other properties of nanotubes such as composition, annealing characteristics, and specific surface. In our experiments, the purification process with 0.1M HCl solution altered the intensities of the peaks in the XRD pattern, shown in Figure 1c, due to changes in the titanate structure. These changes occurred because the nanotubes exchanged Na ions with the HCl solution as observed in the EDS results (Figure 5). These results are in accordance with those reported by Poudel et al. [29] who considered that the purification process is required for the formation of high purity nanotubes. Thus, the purification process influences the formation of nanotubes and the hydrothermal treatment affects their structural composition [30].

Formation of nanotubes after the purification process was observed from TEM results (Figure 6). From the histogram (Figure 7) the average inner diameter was determined as 7.5 nm, the external diameter as 8.4 nm and the length as 34 nm.

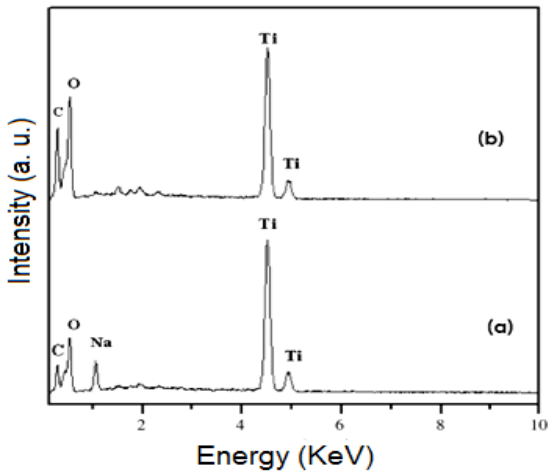

Fig. 5. EDS spectra of nanotubes (a) after hydrothermal treatment without purification process, (b) after purification process.

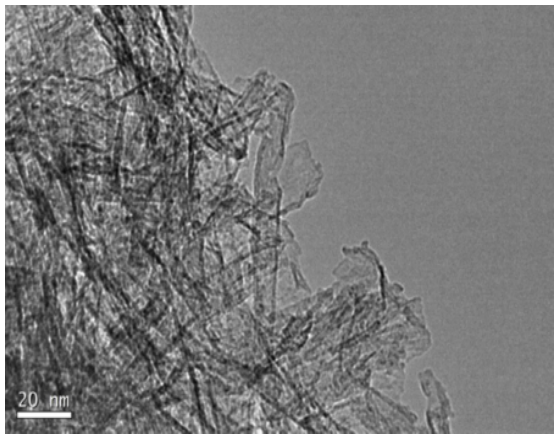

Fig. 6. TEM micrograph of the nanotubes formation, after the hydrothermal treatment at 110^{o}C and the purification process with 0.1 M HCl solution.

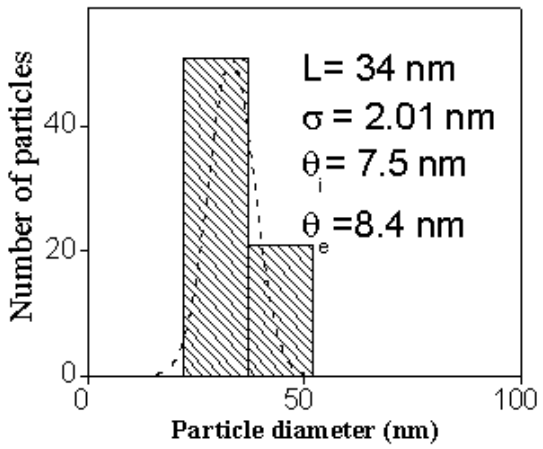

Fig. 7. Distribution of the average size of the nanotubes after the purification process.

Figure 8 presents the results of the TEM analysis of the nanotubes after the annealing treatment at 400°C. As seen, the tubular morphology did not change. According to the histogram shown in Figure 9, the characteristics of the nanotubes were, inner diameter: 7.2 nm, outer diameter: 8.1 nm, length: 30 nm. This result was similar to that calculated from XRD analysis in Figure 1d.

As mentioned above, in section 3.1, when nanotubes were annealed at 800 °C (Figure 1f) the crystalline structure changed from the anatase phase to the rutile phase. This change was confirmed by the TEM analysis shown in Figure 10; as seen, nanotubes morphology disappeared to form nanoparticles with average diameter of 116 nm (Figure 11), greater than the one of the precursor material. Similar results are reported by *Sreekantan et al* [31,32]. They observed that high annealing temperature contributes to the collapse of nanotubes due to the evaporation of hydroxyl groups. Reduction of the number of hydrogen bonds causes the destruction of nanotubes forming nanoparticles with large dimensions.

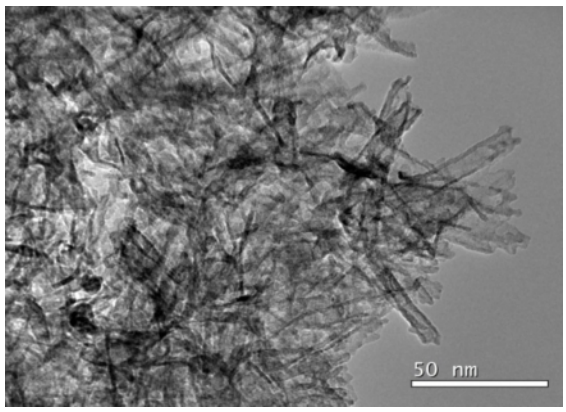

Fig. 8. TEM micrographs of TiO_2 nanotubes annealed at 400 °C.

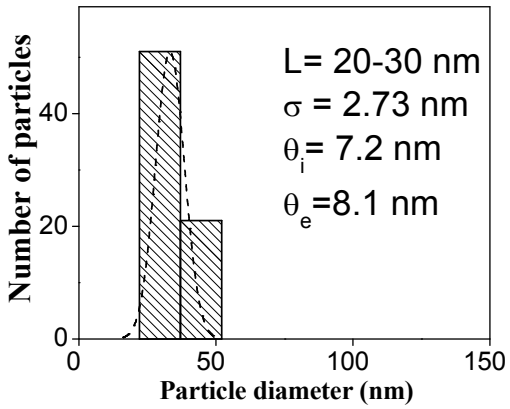

Fig. 9. Length of the nanotubes annealed at 400°C.

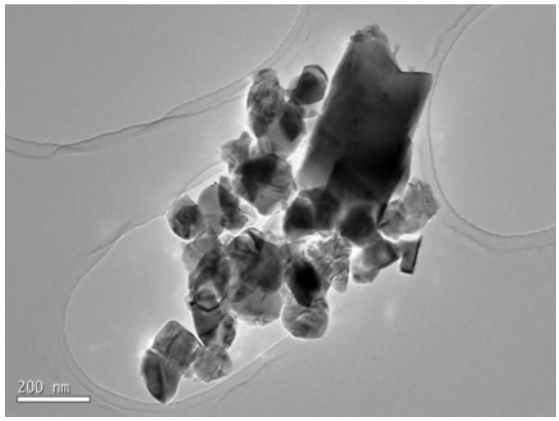

Fig. 10. TEM micrographs. Nanoparticles formed after annealing nanotubes at 800 °C.

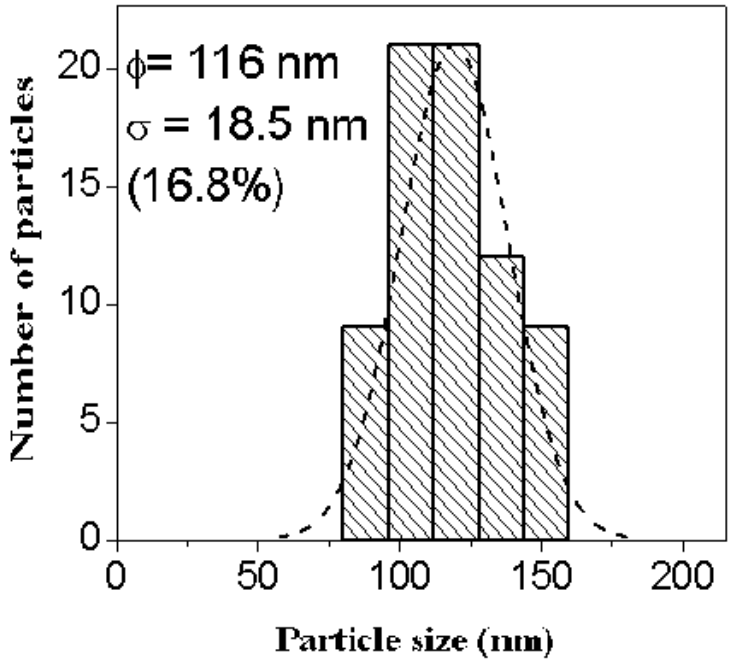

Fig. 11. Diameter of nanoparticles formed after annealing nanotubes at 800°C.

Table 1. Physical properties of the chemical reagents

Reagent	Formula	M_W (g/mol)	Purity (%)	Provider
Degussa P25	TiO_2	79.87	≥99.5	Aldrich
Sodium Hydroxide	NaOH	40	99.1	Baker
Hydroclorhydric acid	HCl	36.46	99,7	Baker
Distilled water	H_2O	18.01	18 Ω	Millipore

Table 2. Summarizes the results of nanotubes characterization via TEM and XRD

Figure	Morphology (TEM)	Structure (XRD)	Average size (nm)
1a	Irregular	Anatase	20
1b	Nanosheet	Orthorhombic [ii]	30
1c	Nanotube	Anatase	Di=7, De= 8, L= 30
1d	Nanotube	Anatase	Di = 7, De = 8, L = 30
1e	Irregular	Rutile	120

CONCLUSION

The effect of the hydrothermal treatment, the purification process and the annealing temperature on the formation process, the structure and the morphology of TiO_2 nanotubes was investigated. From the EDS, XRD and the TEM analysis, it can be concluded that

a) The hydrothermal treatment of the precursor nanoparticles of TiO_2 and the purification process with a HCl solution are essential to form and define the structure of nanotubes. The hydrothermal treatment induces a change in the crystalline structure of the precursor nanoparticles from anatase phase to an orthorhombic phase which characterizes the titanate structure. The purification process contributes to the formation of high purity nanotubes due to Na ions exchanged from the titanate structure to the HCl solution.
b) The annealing temperature influences the morphology and dimensions of nanotubes structure. Annealing temperatures in the range of 400^{o}C and 600^{o}C are optimum to maintain a very stable tubular morphology of nanotubes. Temperatures greater than 600^{o}C change the morphology of nanotubes from tubular to an irregular structure of nanoparticles with a size bigger than that of the precursor material, i.e., the crystalline structure changes from anatase phase to rutile phase causing the destruction of the nanotubes.

REFERENCES

[1]. G. K. Mor, M. A. Carvalho, O. K. Varghese, M. V. Pishko and C. A. Grimes, J. Mater. Res. 19 (2004), 628
[2]. Z.R. Tian, J.A. Voigt, J. Liu, B. McKenzie, H. Xu, J. Am. Chem. Soc. 125 (2003) 12384
[3]. A. L. Linsebigler, G. Lu, J. T. Yates, Jr. Chem. Rev. 95 (1995) 735.
[4]. Y. Lei, L. D. Zhang, G. W. Meng, G. H. Li, X. Y. Zhang, C. H. Liang, S. X. Chen Wand Wang, Appl. Phys. Lett. 78 (2001) 1125.
[5]. K. Varghese, D. Gong, M. Paulose, C. A. Grimes, E. C. J. Dickey, Mater. Res. 18 (2003) 156.
[6]. M. Adachi, Y. Murata, I. Okada, S. J. Yoshikawa, Electrochem. Soc. 150 (2003) G488.
[7]. T, Kasuga, M, Hiramatsu, A, Hoson, T. Sekino and K. Nihara, Langmuir. 14 (1998) 3160.
[8]. B.X. Wang, D.F. Xue, Y. Shi, F.H. Xue, Schwartz W.V., A.I. (Eds.). Nanorods, Nanotubes and Nanomaterials Research Progress. New Nova Science Publishers Inc. (2008) 163:201.
[9]. K. Kiatkittipong, J. Scott, R. Amal. ACS Appl. Mater. Interfaces 3 (2011) 3988.
[10]. B. Vijayan, N. Dimitrijevic, T. Rajh, K.A. Gray. Jour. Phys. Chem. C, (2010) 12994.
[11]. JCPDS Powder Diffraction File, (Swarthmore, PA: JCPDS, International Center for Diffraction Data (1980). Card 21-1272.
[12]. B. Vijayan, N. Dimitrijevic, T. Rajh, K.A. Gray. Jour. Phys. Chem. C, (2010) 12994–13002.
[13]. N. Harsha, K.R. Ranya, K.B. Babitha, S. Shukla, S. Biju, M.L.P. Reddy, K.G.K. Warrier. Journal of Nanoscience and Nanotechnology. 11 (2011) 1175.
[14]. JCPDS Powder Diffraction File, Swarthmore, PA: JCPDS, International Center for Diffraction Data (1980). Card 01-086-0148.

[15]. Y-Q. Wang, G-Q. Hu, X-F. Duan, H-L. Sun, Q-K. Xue, Chem Phy Lett. 365 (2002) 427.
[16]. G.H. Du, Q. Chen, R.C. Che, Z.Y. Yuan, L.M. Peng, Appl. Phys. Lett. 79 (2001) 3702.
[17]. X.M. Sun, Y.D. Li, Chem. Eur. J. 9 (2003) 2229.
[18]. T. Kasuga, M. Hiramatsu, A. Hoson, Sekino, Nihara T, K. Adv. Mater. 11 (1999) 1307.
[19]. D.S. Seo, J.K. Lee, H. Kim, J. Cryst. Growth. 229 (2001) 428.
[20]. Y. Q. Wang, G. Q. Hu, X. F. Duan, H. L. Sun, Q. K. Xue, Chem Phy Lett. 365 (2002) 427.
[21]. Q.H. Zhang, L. Gao, J. Sun, S. Zheng, Chem Lett. 226 (2002) 227.
[22]. Y. Zhu, H. Li, Y. Koltypin, Y. R. Hacohen, A. Gedanken, Chem Commun. 24 (2001) 2616.
[23]. W. Mingdeng, Y. Konishi, H. Arakawa. J. Mater. Sci. 42 (2007) 529:533.
[24]. Y. Q. Wang, G. Q. Hu, X. F. Duan, H. L. Sun, Q. K. Xue, Chem Phy Lett. 365 (2002) 427.
[25]. B. Poudel, W. Z. Wang, C. Dames, J. Y. Huang, S. Kunwar, D. Z. Wang, D. Banerjee, G. Chen, Z.F. Ren, Nanotechnol. 16 (2005) 1935.
[26]. B. X. Wang, D. F. Xue, Y. Shi, F.H. Xue A.I. Nanorods, Nanotubes and Nanomaterials Research Progress. 163 (2008) 201.
[27]. S. Sreekantan, C.W. Lai, J. Alloys Comp. 490 (2010) 436.